Characteristics of historical debris avalanche in the Sedorongpu Basin

Zonglin Tu[1], Zhe Chen[1], Xiaojiang Wang[1], Zhiqing Ye[1], Shuang Luo[2*]

[1] The 7th Geological Brigade of Sichuan Province, Leshan, Sichuan, 614000, China
[2] College of Water Conservancy and Hydropower, Sichuan Agricultural University, Ya'an, Sichaun, 625014, China

*Corresponding author's e-mail: 2682091224@qq.com

Abstract. Because of its unique geographical environment and special climatic conditions, the Sedorongpu basin experiences frequent glacial geological hazards. This study focuses on the characteristics of a recent large-scale debris avalanche disaster (October 17, 2018) in the Sedorongpu Basin, aiming to investigate the characteristics of the debris avalanche, and the conclusions are as follows: (1) The duration of the ice-rock debris avalanche movement is approximately 500 s, with a travel distance of 1 km. During the movement, influenced by the geographical conditions, the speed of the debris flow exhibits a bimodal pattern along the course. The maximum velocity reaches 28 m/s in the initiation zone, while the second peak occurs near a tongue in the gully, with a speed of around 20 m/s. (2) The entrainment and scouring effect of the avalanche material on the gully deposits is evident and varies along the course. The upper section of the gully deposits experienced significant scouring, with a depth of up to 30 m. In contrast, the thickness variation of the lower section deposits is only about 10 m. (3) The ice-rock debris avalanche accumulates at the valley mouth, forming a dam that obstructes the main stem of the Yarlung Tsangpo River. The dam has a length of 2715 m and a height of 98 m, with a volume of 66 million m³. In summary, the model established in this study has high applicability to the Sedorongpu Basin. It can provide a reference for the inversion and prediction of similar disasters in the future.

Keywords: Sedorongpu Basin; numerical simulation; debris avalanche; movement characteristics

1 Introduction

Due to accelerated global climate change, various natural disasters caused by extreme weather events have become more frequent. Glacier-related geohazards have attracted significant research attention due to their strong climate sensitivity and complex internal mechanisms[1,2]. Glacier-related geohazards encompass a wide range of types, including ice-rock avalanches, ice-rock debris avalanches, glacier-dammed lakes, glacier-dammed lake outbursts, and combinations of multiple hazards[3]. These hazards

D. Li et al. (eds.), *Proceedings of the 2023 9th International Conference on Architectural, Civil and Hydraulic Engineering (ICACHE 2023)*, Advances in Engineering Research 228,
https://doi.org/10.2991/978-94-6463-336-8_53

often result in large-scale disasters. According to the statistics, there are 737 cases of glacier collapses and 80 cases of glacial lake outburst floods worldwide between 1901 and 2019[4]. On April 7, 2012, an ice-rock avalanche occurred in the Siachen Glacier disputed region, destroying the Gayari base in Pakistan and causing the deaths of 138 soldiers[5]. In 2015, an ice-rock avalanche buried a village in Langtang, resulting in the deaths of more than 350 people[6].

The Sedorongpu Basin is located in the largest modern glacier distribution area in the mid-low latitudes, the southeastern part of the Qinghai-Tibet Plateau. Since of the presence of glaciers and intense freeze-thaw weathering, the basin has experienced frequent ice-rock debris avalanche disasters throughout history, with at least 14 occurrences between 2014 and 2019[7–9]. Among them, a large-scale ice-rock debris flow event on October 17, 2018, blocked the main stream of the Yarlung Tsangpo River, creating a barrier lake[10,11]. This event posed a significant threat to residents and transportation in the upstream and downstream areas, attracting the attention of scholars. Liu (2021) analyzed the deformation of glaciers in the Sedorongpu Basin over multiple years using Interferometric Synthetic Aperture Radar (InSAR) technology and found that the deformation of glaciers in the basin was mainly subsidence. Before the ice-rock avalanche occurred, there were no signs of accelerated deformation in the avalanche area, and the ground deformation in the flow area was not significant before and after the avalanche, while the ground in the accumulation area showed an initial rise followed by subsidence[12]. Liu (2019) analyzed the movement process and river-blocking effect of this debris avalanche event based on field investigation data and image interpretation. The study suggested that this disaster was caused by a combination of specific geographical conditions, abundant sediment supply, ample precipitation, and active tectonic movements. It also proposed the possibility of future ice-rock debris avalanches under certain conditions[13]. Huai (2022) integrated multi-year remote sensing imagery, geographic information data, seismic records, and climate conditions in the Sedorongpu Basin to determine that the regional topography and climate background are fundamental factors in the periodic occurrence of ice-rock debris avalanche hazards in the basin. The study also proposed an evaluative approach for glacier hazards in the area[14].

This research utilizes field investigation data and relevant historical materials to analyze the movement and accumulation characteristics of the ice-rock debris avalanche blockage event that occurred in Sedorongpu Basin on October 17, 2018. The findings aim to provide reference for future disaster prevention and mitigation in the region.

2 Study area

2.1 Environment

The Sedorongpu Basin (29°45'1.47 "N, 94°56'14.37 "E) is located in Milin County, Tibet Autonomous Region, and it is a primary tributary on the left bank of the Yarlung Tsangpo River. The total area of the watershed in the study area is 66.8 km^2, with a main gully length of approximately 12.5 km. The highest point of the gully is at an elevation of 7283 m, while the lowest point at the gully mouth is at an elevation of 2724 m, resulting in a total elevation difference of 4559 m, with an average slope gradient of about 365‰. The gully has steep upper reaches and gentle lower reaches, with the basin area with slopes greater than 30° accounting for 61.6% of the total area. The watershed is characterized by extensive glacier development, with a year-round glacier area of 23.6 km^2, which represents approximately 35% of the total area. The region is situated along the pathway of the Indian monsoon entering the Qinghai-Tibet Plateau. The climate belongs to the high plateau temperate semi-humid monsoon climate zone, characterized by abundant rainfall, with an average annual precipitation of approximately 1100 mm. The rainy season coincides with the warm season, resulting in high evaporation rates. The morphology of the gully exhibits a "leaf" shape and is primarily composed of one main gully (#1) and four tributaries (#2, #3, #4, #5) (Figure 1). The upper reaches of the main gully and the tributary valleys exhibit a wide, "U" shape. The glacier zone has slopes mostly exceeding 40°, which facilitates the accumulation of rainwater and the occurrence of ice avalanches. The lower slopes are characterized by ice funnels and ice tongues, providing favorable conditions for the accumulation of loose solid materials. The lower reache of the main gully is a deep-cut "V"-shaped valley, where the erosive effects of water flow and debris flows are strong. The gully mouth is connected with the Yarlung Tsangpo River valley, which is a wide valley of the river, with a gully width of 500-700m, and a longitudinal slope of the river of 6-10‰ conducive to the accumulation of the debris avalanche materials.

2.2 Debris avalanche on October 17, 2018

On October 17, 2018, a large-scale ice avalanche occurred at an elevation of approximately 5500 meters above main gully #1(Figure 2, Figure 3). After the glacier was triggered, it started moving rapidly downstream along the main gully. A significant amount of historical glacial debris located on the gentle slope at an elevation of 4000 meters was scoured and entrained by the avalanche material, reaching depths of several tens of meters. At this point, the ice (rock) avalanche mixed with the accumulated debris, forming an ice-rock debris avalanche that continued to travel down the main gully. As the ice-rock debris avalanche reached the circulation zone, it continued to erode and scour the sediment within the gully, eventually reaching a gentle section near the outlet of the Yarlung Tsangpo River and forming a dam, obstructing the flow. This dam created a barrier lake with a storage capacity of approximately 150 million m^3, causing the water level upstream to rise by 40 m and inundating an area up to 27 km away. The event led to the displacement of 16,600 people, damage to 0.34 km^2 of farmland, and an economic loss of 300 million.

Fig. 1. Location of the Sedorongpu Basin

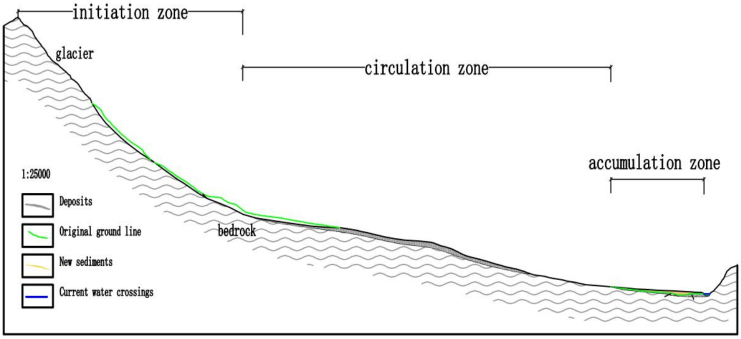

Fig. 2. Profile of the main gully

Fig. 3. Geomorphological map of the subregion (From left to right: initiation zone, circulation zone, accumulation zone)

3 Methodology

3.1 Research Method

Combining similar studies and scale effects, this paper adopts the discrete element method (DEM) to carry out the inversion of the Sedorongpu ice-rock debris avalanche. The Particle Flow Code3D software (PFC3D) is used to solve the problem of granular unit materials originally. With the rapid advances in computer technology, a variety of customized contact models have been developed to simulate the motion and deformation of particles under large-scale continuous action. Thus, this study selectes the PFC3D for numerical simulation.

PFC3D primarily employs modules for particle motion, contact interactions, and wall contacts to establish physical scenarios. Through iterative computations, the model reaches equilibrium state and provides convergent solutions for particle motion parameters. In this study, a geometric wall unit is used to establish the basin topography model, and particle interaction contact is used as the evolution of motion. Considering the channel deposits' consolidation effect, a contact bonding model is selected. The interactions between the avalanche and the gully deposits, as well as the debris avalanche and the gully, are modeled with rigid (linear) contacts[13,15]. Additionally, a computational fluid dynamics module is incorporated into the PFC3D for simulating the entire process from the ice-rock avalanche area to the Yarlung Tsangpo River blockage. This analysis provided analysis and support for assessing the extent of the disaster chain.

3.2 Research approach:

The study uses high-resolution elevation data of the Sedorongpu Basin to generate a topography model at a 1:1 scale (Figure 4). Combined with field survey data and relevant research [16], particle-particle, particle-ground, and particle-water interactions models are established. The movement process of the ice-rock debris avalanche on October 17, 2018, is then inversely simulated using a trial and error approach. The specific settings are as follows: (1) In the circulation zone, particle deposits with a certain thickness (approximately 30m) and porosity (0.45) are generated based on survey data, and a damping coefficient ia applied to accelerate their compression and achieve stable consolidation. (2) Accounting for the average flow velocity and water depth observed over several years in the Yarlung Tsangpo River, an average flow velocity of 1.25 m/s is set, with a water depth of 5-10 m at the gully mouth. (3) In the initiation area, particle sources of different volumes are generated, while the morphology and porosity are same as the avalanche zone. And they initiate to slide under the influence of gravity, simulating the ice (rock) avalanche. (4) Fourteen measurement points are established along the main gully to observe the characteristics of the debris avalanche (Figure 4). Finally the optimal combination of numerical simulation parameters is presented in Table 1.

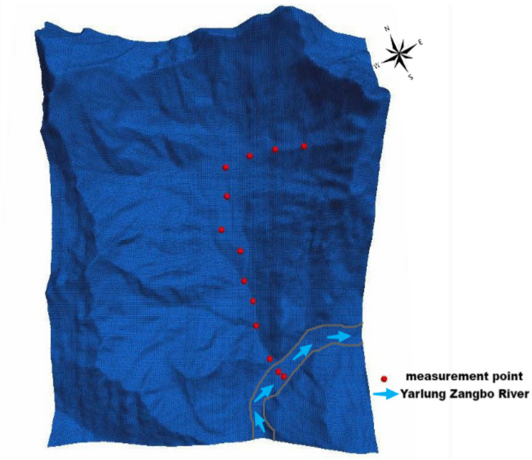

Fig. 4. 3D topographic map of the Sedorongpu Basin

Table 1. Parameters of the numerical simulation

Parameter	Value
Contact model	Linear contact bond model
Bonding strength (Pa)	cb-tenf: 0.98×10^{10} cb-shear: 1.02×10^{13}
Contact model in motion	Linear Model
Ball density (kg/m^3)	2200~2500
Stiffness (N/m)	k_n: 1.12×10^{10} $k_{s:}$ 1.13×10^7
Coefficient friction	Static: 0.99 Kinetic: 0.09
Damping factor	0.11

4 Result

4.1 The motion characteristics

The process of the ice-rock debris avalanche disaster on October 17, 2018, obtained through the inverse analysis using the PFC3D, is shown in the Figure 5. At t=0s, the ice (rock) avalanche from the high-altitude glacier above the main gully begins to move downward. At this time, the volume of the avalanche is small, and the velocity starts to increase. At t=7s, the ice (rock) avalanche contacts the deposits in the gully, and the velocity reaches dozens of meters per second. At t=100s, the upper gully deposits become unstable and move downward due to the scour and entrainment effects of the avalanche materials, forming an ice-rock debris avalanche. At this point, the flow velocity of the debris avalanche decreases due to internal dissipation and the decrease in slope. At t=200s, more gully deposits participate in the movement, the volume of the ice-rock debris avalanche increases, and because of the presence of a topographic inflection zone (ice tongue) in the gully, the velocity of the ice-rock debris avalanche increases again. At t=253s, the ice-rock debris avalanche reaches the mouth of the gully, about to join the Yarlung Zangbo River. At t=500s, the main body of the ice-rock debris avalanche is obstructed by the gully and the opposite bank, stops moving, and forms a dam, and the movement ends. The entire movement process lasts for 500s, covering a distance of 10km, with an average velocity of 20m/s.

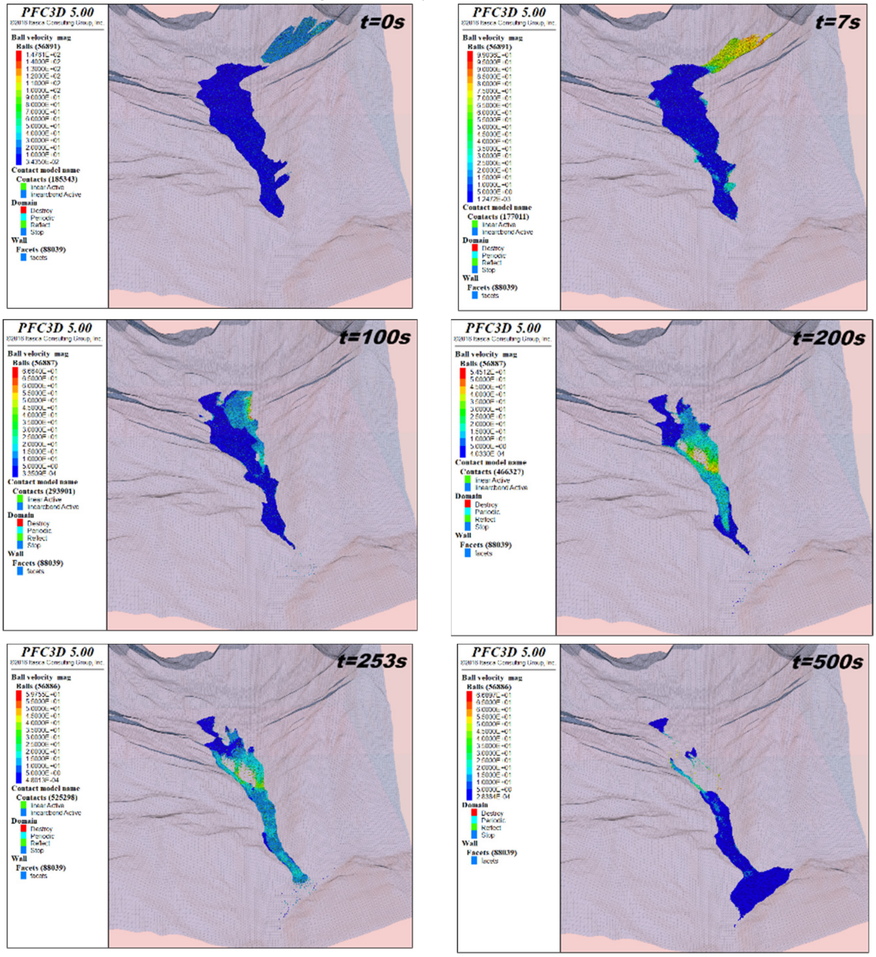

Fig. 5. Time-lapse image of deposit distribution during the debris avalanche

The distribution of the maximum velocity along the path during the motion of the ice-rock debris avalanche is shown in the Figure 6. It can be observed that the velocity of the ice-rock debris avalanche varies significantly due to the topography during the entire movement process. The maximum velocity values along the path exhibits a bimodal distribution. After the ice (rock) avalanche, the potential energy is transformed into kinetic energy, and the velocity reaches 27m/s in the initiation area. After passing measurement point 3, the velocity of the debris flow continues to decrease owing to the decrease in slope and the obstruction of gully deposits, dropping to 6m/s at measurement point 6. Measurement point 7 represents the ice tongue in the main gully. When the ice-rock debris flow reaches this point, there is a sudden change in topography, and the velocity exceeds 20m/s. After the ice-rock debris avalanche reaches the deposition area, the movement gradually stops and forms a dam blocking the Yarlung Zangbo River.

To study the entrainment and deposition characteristics of the debris avalanche, the variation of mud depth at measurement points 4 and 6 (in the initiation zone) and measurement point 11 (in the accumulation zone) during the motion of the ice-rock debris flow is investigated, as shown in the Figure 7. Measurement point 4 is located in the upper section of the circulation zone, where there is a large amount of loose ice-carrying deposits left by early debris avalanches, with a deposit thickness of up to 25m. 40s after the ice avalanche, the avalanche materials reache measuring point 4, causing a rapid increase in mud depth in a short period of time. Subsequently, the debris flow scours and entrains the ice-carrying deposits, and the mud depth at measuring point 4 gradually decreases to 0 within 240s. All the ice-carrying deposits at this location is involved in the movement of the debris avalanche. Measurement point 6 is located in the lower circulation zone, and the variation in mud depth is similar to that at measuring point 4. It firstly increases and then decreases, but the deposits at this location is not completely eroded by the debris avalanche. When motion ends, there still remains a thickness of approximately 10 m. Measurement point 11 is located at the intersection of the Sedorongpu main gully and the Yarlung Zangbo River. The mud depth at this point increases after 150s of the ice (rock) avalanche, and this is due to the disturbance caused by the scour and entrainment of the upper part of the channel deposits by the sliding mass, which is transported downward through internal particle conveyance, causing instability in the lower part of the channel deposits. The leading material of the ice-rock debris avalanche reaches this point at around 250s. At 350s, the main body of the debris avalanche rushes out of the gully mouth, and the mud depth at measuring point 11 rapidly increases to about 80m and stabilizes.

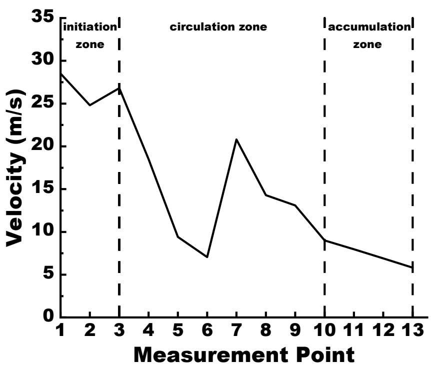

Fig. 6. Maximum velocity distribution curve along the course

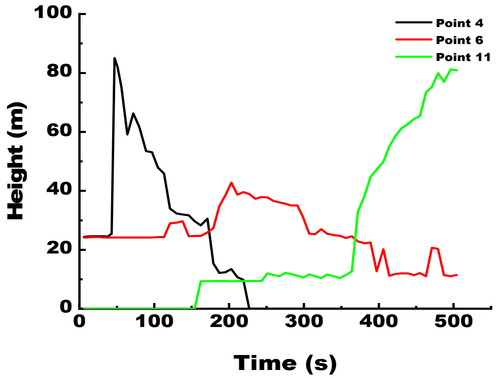

Fig. 7. The depth variation curve at different measuring points

4.2 Deposition characteristics

The morphology of the ice-rock debris avalanche deposit obtained through numerical inversion is shown in Figure 6. The deposit exhibits a "fish-tail" shape, and a comparison of its inversion results with investigation values[13,15–18] is presented in Table 2. From the table, it can be observed that the dam resulting from this disaster has a length along the river of 2715 m, a height of 98.7 m, and a volume of 6.9×10^7 m^3. These values are larger than the investigation values, but the percentage errors for both indicators are less than 10%. Therefore, the credibility of the results is relatively high.

Table 2. Comparison of inversion results with investigation values

Characterization of the weir	Inversion result	Investigation result	Error
Length (m)	2715	2500	8.60%
Height (m)	98.7	90	9.67%
Volume (m$\times$ $10^7$$m^3$)	6.9	6.6	4.54%

5 Conclusion and discussion

PFC3D is used to invert the ice-rock debris avalanche event in Sedorongpu on October 17, 2018, yielding the following conclusions:

(1) This Sedorongpu debris avalanche event lasts for 500 s and travels a distance of 10 km. During the movement, the maximum velocity of the debris avalanche exhibits a bimodal distribution along the path. The peak value of 28 m/s is observed in the initiation zone, while the second peak value of 22 m/s is influenced by the terrain and appears in the downstream part of the circulation zone.

(2) During the downward movement of debris flow, entrainment by the avalanche scours and scrapes the sediments in the gully, resulting in a thickening and then a thinning of the ice deposits in the flow pathway, eventually converging in the accumulation zone. There are deposits with a thick of approximately 25 m in the upper section of the

main gully, which are strongly affected by avalanche, causing all the deposits participating in the debris avalanche. In the lower section, the entrainment effect is relatively weak, and combined with the gentle terrain, leading to the accumulation of ice debris in this area, with only a portion of it forming the debris avalanche. Hindered by the topography, the ice-rock debris avalanche eventually accumulates in the gully mouth, with a dam height of 98.7 m blocking the main channel of the Yarlung Tsangpo River,.

(3) The numerical model for ice-rock debris avalanche hazards in the Sedorongpu Basin, developed through a trial-and-error approach, demonstrates strong applicability for studying ice-rock debris avalanches in the region. The numerical results of various indicators for this ice-rock debris avalanche exhibit an error of less than 10% compared to the investigation values. This high level of consistency between the model results and the investigation values demonstrates that the model can accurately predict the motion of ice-rock debris avalanches in the Sedorongpu Basin, thereby providing valuable guidance for disaster prevention and mitigation in this area.

Although this study successfully inverts the ice-rock debris avalanche in Sedorongpu Basin, there are still some limitations to be addressed:

(1) The focus of this inversion analysis is on the initiation, formation, and accumulation processes of the ice-rock debris avalanche, but lacks research on the backwater of debris dam and the breaching process of the dam, thus forming an incomplete perspective on the disaster chain.

(2) The numerical model established in this study using the trial-and-error method is based on relevant survey data and similar studies. However, the interactions among the materials within the debris avalanche cannot be thoroughly explored. Further research can consider integrating laboratory shear tests to investigate this aspect.

(3) Sedorongpu Basin is located in a sparsely populated high-altitude area, making it challenging to obtain timely and accurate data during the occurrence of the disaster. This leads to some error in the research for this region. For example, Wang [18] and Hu [8] points out that the disaster occurred in the evening of the 16th (instead of the next early morning as reported by the official Xinhua news). In addition, the estimated scale of the dam varies between 40 and 66 million m^3[10,11,17] without a definitive value. Hence, there is an urgent need to improve disaster monitoring methods for the Sedorongpu Basin and similar regions.

Acknowledgments

This study is supported by the scientific research program (2023-4) of the 7th Geological Brigade of Sichuan Province.

Reference

1. Yao X, Iqbal J, L LJ, Zhou ZK. (2019) Characteristics of mountain glacier surge hazard: learning from a surge event in NE Pamir, China. Journal of Mountain Science, 16(7): 1515–1533.

2. Ji Q. (2018) GLACIER VARIATIONS IN RESPONSE TO CLIMATE CHANGE IN THE HIMALAYA DURING 1990-2015. Lanzhou University.
3. Bajracharya S R, Mool P. (2009) Glaciers, glacial lakes and glacial lake outburst floods in the Mount Everest region, Nepal. Annals of Glaciology, 50(53): 81–86.
4. Zhang TG, Wang WC. (2022) Global inventory of glacier-related slope failures and moraine dammed lake outburst floods (1901-2020). https://poles.tpdc.ac.cn/zh-hans/data/3ecd6ef8-fb24-44f0-b9f1-c8839fe83760/?q=.
5. Tong LQ, Pei LX, Tu JN, Guo ZC, Yu JK, Fan JH, Li DD. (2020) A preliminary study of definition and classification of ice avalanche in the Tibetan Plateau region. Remote Sensing for Natural Resources, 32(2): 11–18.
6. Zhang TT, Yin YP, Li B, Liu XJ, Wang M, Gao Y, Wan JW, Gnyawali K R. (2023) Characteristics and dynamic analysis of the February 2021 long-runout disaster chain triggered by massive rock and ice avalanche at Chamoli, Indian Himalaya. Journal of Rock Mechanics and Geotechnical Engineering, 15(2): 296–308.
7. Yang C. (2019) Evolution characteristics and formation mechanism of the Glacier avalanche - debris flow Events in Sedongpu Gully, Yarlung Zangbo River, Tibet. Chengdu University of Technology.
8. Hu KH, Zhang XP, You Y, Hu XD, Liu WM, Li Y. (2019) Landslides and dammed lakes triggered by the 2017 Ms6.9 Milin earthquake in the Tsangpo gorge. Landslides, 16(5): 993–1001.
9. Chu D, Caiwang DZ, Lawang DZ, Suolang TJ, Pingcuo SD, Duoji ZX, Mingma CR, Ping C. (2022) Monitoring Glacier Avalanches in Tibet Using Sentinel-2 Imagery. Remote Sensing Technology and Application, 37(6): 1289–1301.
10. Chen C, Zhang L, Xiao T, He J. (2020) Barrier lake bursting and flood routing in the Yarlung Tsangpo Grand Canyon in October 2018. Journal of Hydrology, 583: 124603.
11. Jin XP. (2019) Reviews and reflections on emergency response countermeasures for barrier lakes in Jinsha River and Yarlung Zangbo River. Yangtze River, 50(3): 5-9+46.
12. Liu Y, Shi ZT. (2021) Study on the Surface Deformation of lce Avalanche Debris Flow Movement Area in Sedongpu Basin of Yarlung Zangbo River Based on Time Series InSAR. Journal of Yunnan Normal University (Natural Sciences Edition), 41(6): 63–70.
13. Liu CZ, Lv JT, Tong LQ, Chen HQ, Liu QQ, Xiao RH, Tu JN. (2019) Research on glacial/rock fall-landslide-debris flows in Sedongpu basin along Yarlung Zangbo River in Tibet. Geology in China, 46(2): 219–234.
14. Huai BJ, Ding MH, Ai ST, Sun WJ, Wang YT, Gao JJ. (2022) Glacial Debris Flow Blockage Event (2018) in the Sedongpu Basin of the Yarlung Zangbo River, China: Occurrence Factors and Its Implications. Land, 11(8): 1217.
15. Chen LZ. (2016) THREE-DIMENSIONAL NUMERICAL SIMULATION OFYIGONG ROCK AVALANCHEUSING PARTICLE FLOW CODE. Southwest Jiaotong University.
16. Li KZ, Zhang MZ, Xing AG. (2021) Numerical runout modeling and dynamic analysis of the ice avalanche-debris flow in Sedongpu Basin along Yarlung Zangbo River in Tibet.The Chinese Journal of Geological Hazard and Control, 32(1): 18–27.
17. Tong LQ, Tu JN, Pei LX, Guo ZC, Zheng XW, Fan JH, Zhong C, Liu CL, Wang SS, He P, Chen H. (2018) PRELIMINARY DISCUSSION OF THE FREQUENTLY DEBRIS FLOW EVENTS IN SEDONGPU BASIN AT GYALAPERI PEAK, YARLUNGZANGBO RIVER. Journal of Engineering Geology, 26(6): 1552–1561.
18. Wang W, Yang J, Wang Y. (2020) Dynamic processes of 2018 Sedongpu landslide in Namcha Barwa–Gyala Peri massif revealed by broadband seismic records. Landslides, 17(2): 409–418.